SciencePG
Science Publishing Group

Research Article

Solution to the Breach of the Dike of Keur Bara KAIRE, Located in the Commune of Notto Diobasse in the Department of Thiès, Senegal

Ndiouga Camara[1, *], Birane Niane[1], Séni Tamba[2]

[1]Geotechnical Department, UFR Engineering Sciences, Iba Der THIAM University of Thiès, Thiès, Sénégal

[2]Civil Engineering Department, Polytechnic School of Thiès, Thiès, Sénégal

Abstract

This article studies the rupture of the Keur Bara KAIRE dike, located in the commune of Notto Diobasse in the department of Thiès in Senegal. The village is crossed by a stream which collects rainwater from the west to the east, following a natural slope. The overflow of this stream causes serious flooding, leading to the total cutting of the road and the isolation of the population. These floods had tragic consequences, resulting in two losses of human life. To regulate the water level, prevent flooding and protect agricultural and urban areas from overflows, the Senegalese authorities initiated the project to build the Keur Bara KAIRE dike in 2004, unfortunately the latter gave way in 2017. The geotechnical analysis was carried out on samples taken from various points on the site, revealing that the terrain is mainly composed of fine sand and the embankment is made with clayey sand. Morphometric and hydrological investigations highlight that the watershed of the Keur Bara KAIRE dike covers an area of 3.72 km², with a projected flow of 54.99 m³/s. The resizing of the dike revealed the following data: a length of 132 meters and a height of 3 meters. The spillway is 52.99 meters long with a reservoir height of 1.22 meters. The bay walls have a thickness of 50 cm and the embankments have a slope of ½ upstream and downstream. The stability calculation on the broken dike reveals a sliding safety factor (FSG) of 1.84 which complies with the standard and an overturning safety factor (FSR) of 0.13 which is not verified. The surface of the watershed which is equal to 3.72 km², also the smallest height of precipitation is equal to 234.9 mm and the largest 664.4 mm, the ORSTOM and CIEH methods for hydraulic calculations.

1. Introduction

The frequency and intensity of floods have increased in recent decades, largely due to climate change and increasing urbanization [1]. According to the World Food Program (WFP), devastating floods in West and Central Africa have affected five million people in 19 countries in the region.

These floods displaced tens of thousands of people from their homes and decimated more than a million hectares of cultivated land [2]. Senegal is not left out since the country has experienced recurrent floods since 1989. This can be explained by rapid urbanization. The urbanization rate increased

---

from 23% in 1960 to 38.40% in 1988, 40.6% in 2000 and 45.2% in 2013, thus leading to the creation and proliferation of irregular neighborhoods which represent nearly 40% of the total habitat in Senegal, more than 2/3 of which is located in flood zones [3]. Regions like Thiès are particularly affected due to the lawless occupation and topography. It is crucial to understand that flooding varies by region, season and local conditions, and flood responses must be tailored to the specific needs of each region [4]. However, huge investments have been made to build community resilience and build infrastructure. Among these infrastructures, there are protective dikes designed to meet specific needs. In Senegal, after the drought cycle of the 1970s, the Senegalese government invested in the construction of dikes which were used to retain water for agriculture and livestock such as the Allou Kagne 2 dam but also dykes which have the role of protecting populations against flooding such as the Keur Bara KAIRE dike which is the subject of this article. Indeed, this village is crossed by a stream which collects rainwater coming from the West to the East, following a natural slope. The passage of these waters causes serious flooding, literally cutting the road and isolating the population, which resulted in two losses of human life. In response to this situation, in 2004 the Senegalese government undertook the construction of the Keur Bara KAIRE dike, a structure intended to control the water level, prevent flooding, and protect agricultural and urban land from overflows. However, this dike failed in 2017, restoring previous problems. A dike rupture can cause a wave of submersion that is much more dangerous than the flood from which it was supposed to protect populations and its causes can be technical, natural or human. The general objective of this article is to contribute to the protection of populations against flooding by trying to propose a solution to make the dike functional [5].

2. Materials and Methods

2.1. Data Acquisition

The study area is located in the department of Notto Diobass, in the Thiès Region of Senegal. Figure 1 shows the location of the area.
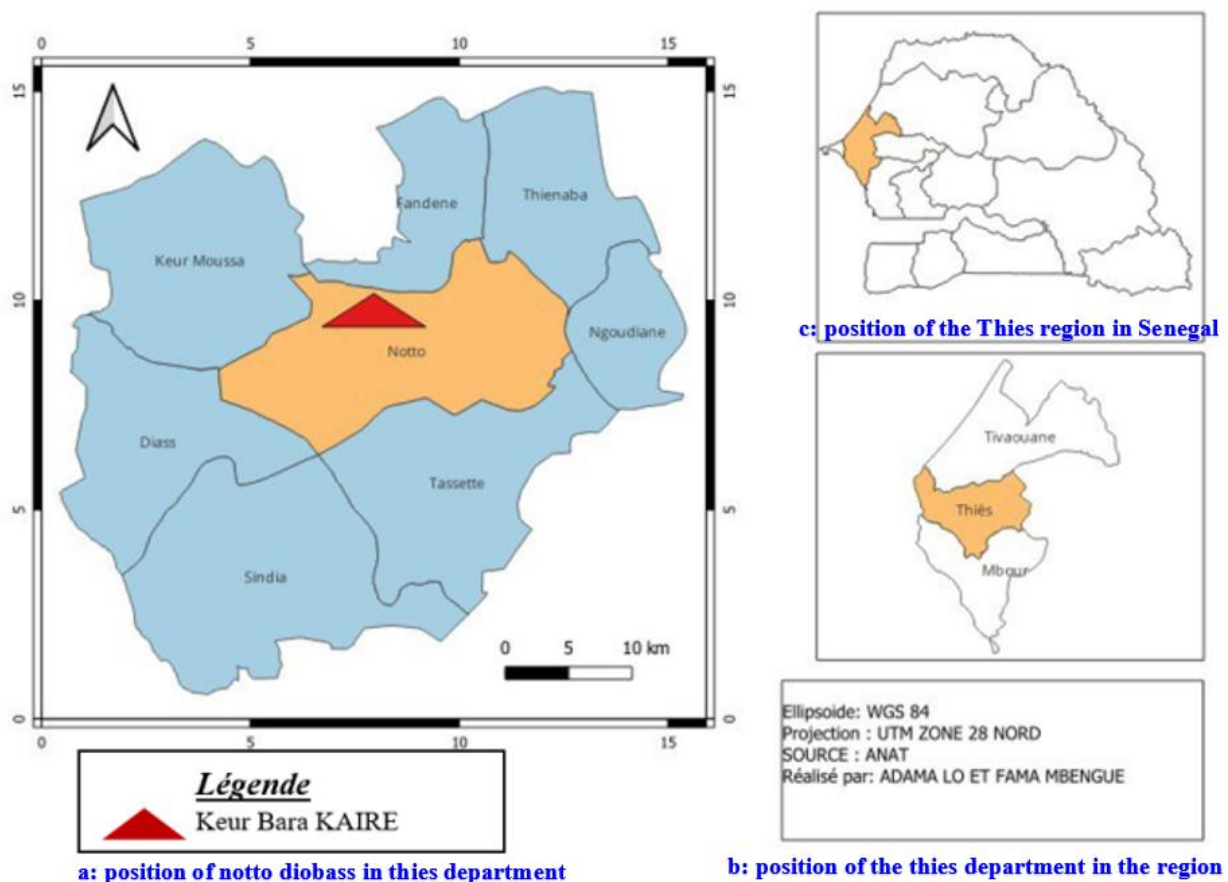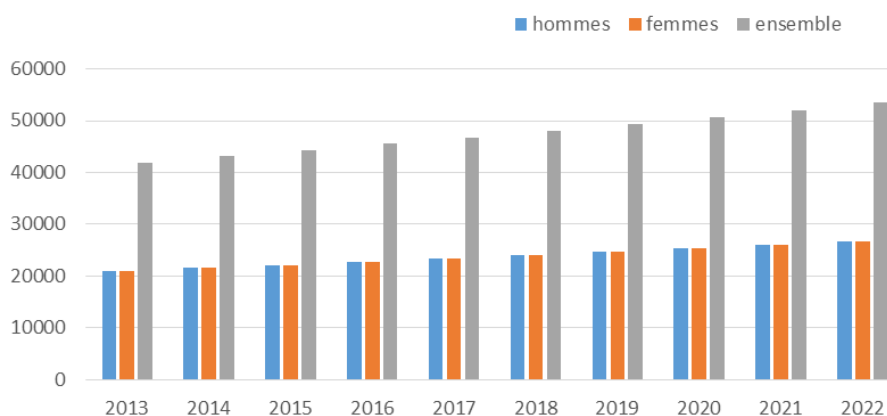

Figure 1. Geographical location of the study area on Qgis.

Figure 2 provides an overview of the study area.
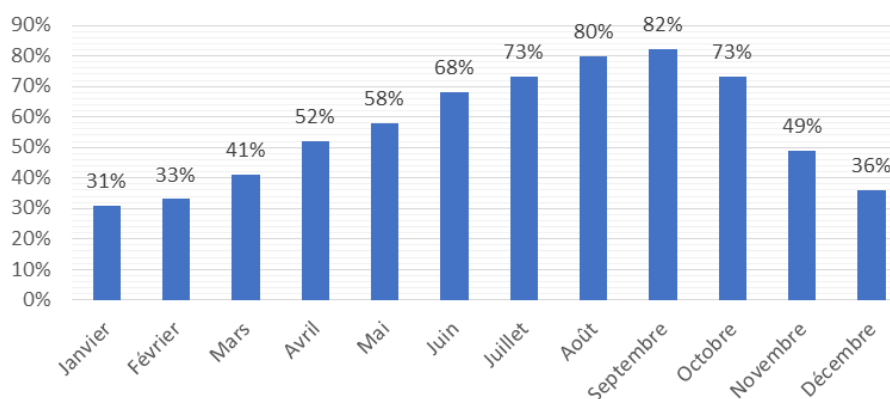
Figure 2. Delimitation of the study area on Google Earth.

The figure 3 shows the evolution of the demographics of the municipality.

Figure 3. the evolution of the demographics of the municipality.

The figure 4 gives a representation of the evolution of humidity in 2021.

Figure 4. Variation of humidity in the Thiès region [3].

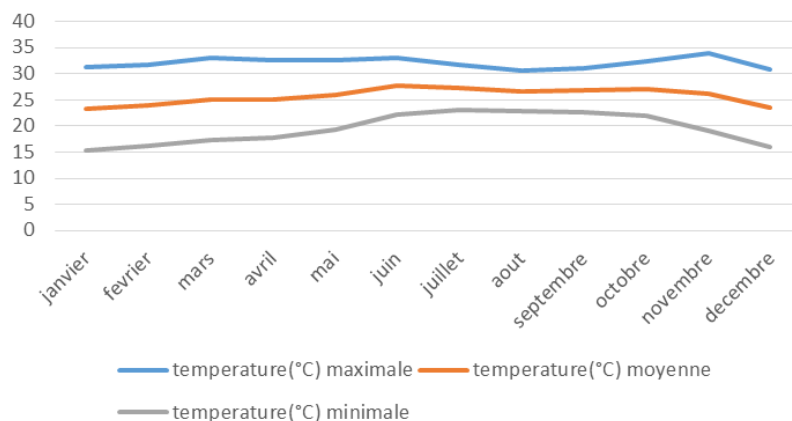The figure 5 shows the temperature variation.

Figure 5. Variation of monthly temperature in the Thies region in 2018 [5].

The winds are moderate and their speeds vary from 2 to 14 m/s. [6] Rainfall follows a sawtooth pattern (figure 6) with an average of around 471 mm per year.
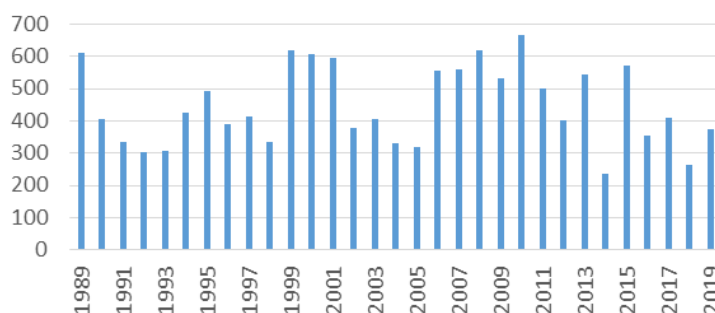
Figure 6. Variation in the average annual rainfall of Thiès from 1989 to 2019 [1].
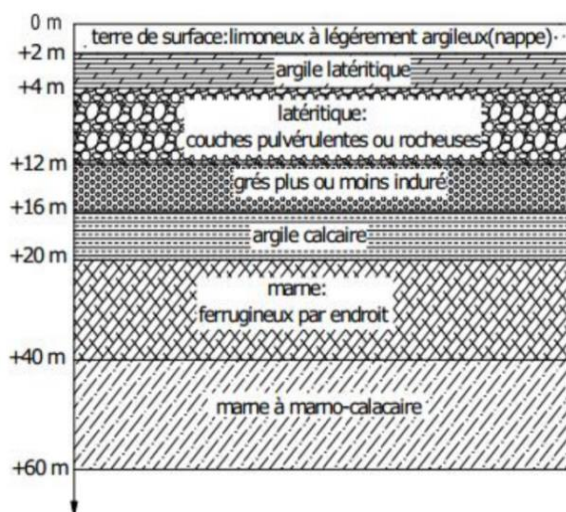
Figure 7. Geological section of Thiès [6].

The morphology of the department causes most of the runoff water to converge towards the lowlands. In other words, the waters leave the highest points (altitude 112 m) towards the lowest (altitude 49 m). This makes the study area, located at an altitude of 82 m, a runoff zone [7].

To characterize the geological structure of Thiès, a section of the different layers was made from the logs of several boreholes as illustrated in Figure 7 [6].

Figures 8-9-10 and 11 illustrate the current state of the Keur Bara KAIRE dike.

Figure 8. Sandbags stored on the track ditch.

Figure 9. Rows of rocks to reduce wave pressure.

Figure 10. Rupture at the down stream slop.

Figure 11. Rupture at the spillway.

Thus, the data obtained makes it possible to follow the procedures and approaches to deal with this specific problem of the dike.

2.2. Data Processing and Analysis [8].

Seven (7) boreholes were made with a depth of 1 m:

Three points upstream,

S1 upstream with coordinates 14°43'51.1" N / 17°4'3.1" W with an altitude of 77m;

S2 upstream with coordinates 14°43'50.2" N/ 17°4'2.4" W with an altitude of 76m;

S3 upstream with coordinates 14°43'49.6" N / 17°4'2.1" W with an altitude of 77m.

Three downstream,

S1 downstream with coordinates 14°43'50" N / 17°4'4.7" W with an altitude of 77m;

S2 downstream with coordinates 14°43'49.2" N / 17°4'3.7" W with an altitude of 77m;

S3 downstream with coordinates 14°43'48.2" N / 17°4'2.9" W with an altitude of 77m.

A point at the embankment of the dike with coordinates 14°43'49" N / 16°55'57" W with an altitude of 77m,

A sample is taken from the protective layer.

An in situ permeability test was carried out to determine the permeability of the soil.

Table 1 gives the permeability classes.

Table 1. Permeability classes depending on the permeability coefficient.

Permeability classes depending on the permeability coefficient	K (m/s)	Degree of permeability
Medium to large gravels	$10^{-1} – 10^{-3}$	Very high
Small Gravel, Sand	$10^{-3} – 10^{-5}$	Quite high
Very fine Sand, silt sand, lœss	$10^{-5} – 10^{-7}$	Weak
Compact silt, clay, loam	$10^{-7} – 10^{-9}$	Very weak
Frank clay	$10^{-9} – 10^{-12}$	Vitually waterproof

GTR classification is a soil classification method used to evaluate soil properties. The GTR classification is made according to the tables in Figures 2 and 3.

Table 2. GTR class A classification.

Classification according to natur				Classification according to water status	
nature parameters First level of classification	Class	nature parameters Second level of classification	Subclass function of nature	Status Settings	State function subclass
Dmax≤50mm and Sieve at	A Sols fins	VBS ≤2,5 ou	A1 Little plastic silts,	IPL≤3 ou Wn≥1,25W$_{OPN}$	A$_1$th
				3<IPL≤8 ou 1,10≤Wn<1,25 W$_{OPN}$	A$_1$h

Classification according to natur				Classification according to water status	
nature parameters First level of classification	Class	nature parameters Second level of classification	Subclass function of nature	Status Settings	State function subclass
$80\mu m>35\%$		$Ip\leq12$	loess, alluvial silts, little polluted fine sands, little plastic arenas	$8<IPL\leq25$ ou $0,9W_{OPN}\leq Wn<1,1W_{OPN}$	A_1m
				$0,7W_{OPN}\leq Wn<0,9W_{OPN}$	A_1s
				$Wn<0,7\ W_{OPN}$	A_1ts
				$IPL\leq2$ ou $Ic\leq0,9$ ou $Wn\geq1,3W_{OPN}$	A_2th
		$12<Ip\leq25$ ou $2,5<VBS\leq6$	A2 Fine clay sands, clay silts and poorly plastic marls, arenas	$2<IPL\leq5$ ou $0,9\leq Ic<1,05$ ou $1,1W_{OPN}\leq Wn<1,3\ W_{OPN}$	A_2h
				$5<IPL<15$ ou $1,05<Ic\leq1,2$ ou $0,9W_{OPN}\leq Wn<1,1W_{OPN}$	A_2m
				$1,2<Ic\leq1,4$ ou $0,7\ W_{OPN}\leq Wn<0,9W_{OPN}$	A_2s
				$Ic>1,3$ ou $Wn<0,7W_{OPN}$	A_2ts
		$25<Ip\leq40$ ou $6<VBS\leq8$	A3 Clays and marly clays, very plastic silts	$IPL<1$ ou $Ic\leq0,8$ ou $Wn\geq1,4W_{OPN}$	A_3th
				$1<IPL<3$ ou $0,8\leq Ic<1$ ou $1,2W_{OPN}\leq Wn<1,4\ W_{OPN}$	A_3h
				$3<IPL<10$ ou $1<Ic\leq1,15$ ou $0,9W_{OPN}\leq Wn<1,2\ W_{OPN}$	A_3m
				$1,15<Ic\leq1,3$ ou $0,7\ W_{OPN}\leq Wn<0,9W_{OPN}$	A_3s
				$Ic>1,3$ ou $Wn<0,7W_{OPN}$	A_3ts
					A_4th
		$Ip>40$ ou $VBS>8$	A4 Very plastic clays and marly clays	Threshold values of state parameters, to be defined in support of a specific study	A_4h
					A_4m
					A_4s

Table 3. GTR class B classification.

CLASSIFICATION TO USE FOR EMPLOYMENT CLASSIFICATION TO USE FOR SHAPE LAYERS							
CLASSIFICATION ACCORDING TO NATURE				CLASSIFICATION ACCORDING TO WATER STATUS		CLASSIFICATION BY BEHAVIOR	
nature parameters First level of classification	Class	nature parameters Second level of classification	Subclass function of nature	Status Settings	State function subclass	behavior settings	Subclass behavior function
$Dmax\leq50mm$ et Sieve at $80\mu m\leq35\%$	B Sols sableux et argileux avec fines	Sieve at $80\mu m\leq12\%$ Sieve at $2mm>70\%0,1\leq VBS\leq0,2$	B1 silite sands	Materials generally insensitive to water		$FS\leq60$	B_{11}
						$FS>60$	B_{12}
		Sieve at $80\mu m\leq12\%$ Sieve at $2mm>70\%$ $VBS>0,2$	B2 Clayey sands (lightly clayey)	$IPL\leq4$ ou $Wn\geq1,25W_{OPN}$	B_2th	$FS\leq60$	$B_{21}th$
						$FS>60$	$B_{22}th$
				$4<IPL\leq8$ ou $1,10\leq Wn<1,25\ W_{OPN}$	B_2h	$FS\leq60$	$B_{21}h$
						$FS>60$	$B_{22}h$

CLASSIFICATION TO USE FOR EMPLOYMENT
CLASSIFICATION TO USE FOR SHAPE LAYERS

CLASSIFICATION ACCORDING TO NATURE				CLASSIFICATION ACCORDING TO WATER STATUS		CLASSIFICATION BY BEHAVIOR	
nature parameters First level of classification	Class	nature parameters Second level of classification	Subclass function of nature	Status Settings	State function subclass	behavior settings	Subclass behavior function
				$0,9W_{OPN} \leq Wn < 1,10W_{OPN}$	B_2 m	FS≤60	B_{21} m
						FS>60	B_{22} m
				$0,5W_{OPN} \leq Wn < 0,9W_{OPN}$	B_2 s	FS≤60	B_{21} s
						FS>60	B_{22} s
				$Wn < 0,5W_{OPN}$	B_2 ts	FS≤60	B_{21} ts
						FS>60	B_{22} ts
		Sieve at 80µm≤12%	B3	Materials generally insensitive to water		LA≤45 et MIDE≤45	B_{31}
		Sieve at 2mm>70%0, 1≤VBS≤0,2	Silty gravel			LA>45 et MIDE>45	B_{32}

For watersheds, their characteristics can vary depending on different factors, such as geology, topography, vegetation, climate and land use [9]. Figure 12 represents the zoning done on Google Earth imported onto Global Mapper.
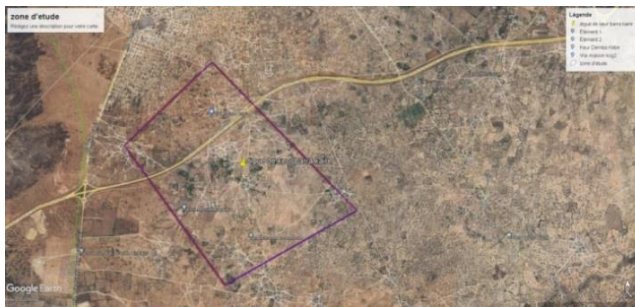

Figure 12. Zoning for watershed delimitation on Google Earth pro.

The design flood calculation is done using the Grésillon formula which allows you to go from the ten-year flood to the hundred-year flood as given in formula 1:

$$Q_{100} = C * Q_{10} \tag{1}$$

Q_{10}: Centennial flow;

C: increase coefficient given by the Gradex method (formula 2):

$$C = 1 + \frac{(P_{100} - P_{10})}{P_{10}} * \frac{\left(\frac{Tb}{24}\right)^{0,12}}{K_{r10}} \tag{2}$$

P_{10}: daily precipitation corresponding to a return period of 10 years;

P_{100}: daily precipitation corresponding to a return period of 100 years;

Tb: basic time (in hours);

K_{r10}: runoff coefficient of the ten-year flood (expressed as a fraction).

For the ratio between centennial and ten-year frequency precipitation:

$$\frac{P_{100} - P_{10}}{P_{10}} = \begin{cases} 0,45 \text{ in the sahelian zone} \\ 0,38 \text{ tropical area} \end{cases}$$

Losses occur through infiltration and evaporation. The methodology adopted for data analysis made it possible to know the shape of the dike, the nature of the soil and to verify the stability of the dik [10].

3. Results and Discussions

The Keur Bara KAIRE watershed is delimited using Global Mapper software. Figure 13 gives the delimitation of the sub-watersheds.
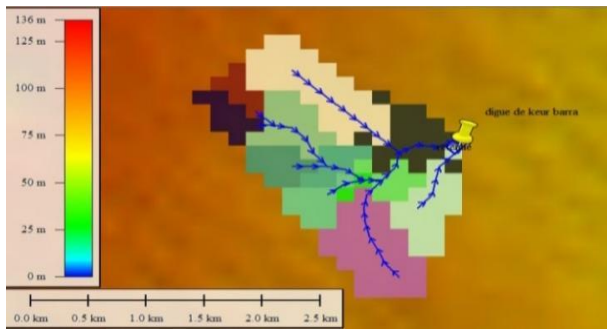
Figure 13. *Demarcation of the sub-watersheds of Keur Bara KAIRE on Global Mapper.*

Figure 14 gives the hypsometric curve of the Keur Bara KAIRE watershed.

Figure 14. *Hypsometric curve of the Keur Bara KAIRE watershed.*

The hypsometric curve made it possible to determine the altitudes at 5% and 95% of cumulative surfaces which are respectively equal to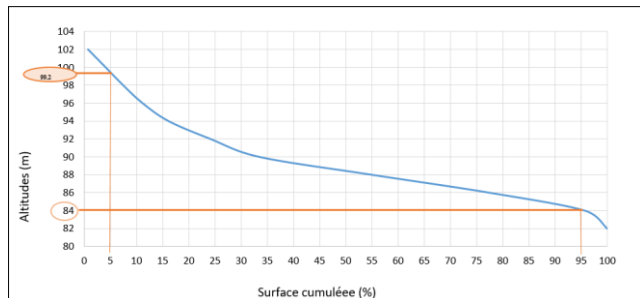 99.2 m and 84 m. These altitudes made it possible to calculate the overall slope index. Table 4 presents the characteristics of the Keur Bara KAIRE watershed.

**Table 4.** *Characteristics of the Keur Bara KAIRE watershed [8].*

Watershed characteristics	Results obtained
Area S in km²	3,72
Perimeter P in km	10,43
Maximum altitude in m	104
Minimum altitude in m	82
Hydraulic length in km	2,54
Average slope	0,63
Shape index KG	1,52
Length of the equivalent rectangle L in km	4,37
Overall slope index Ig in m/km	5,98
Specific height difference Ds in m	11,54
Basin typology	Very small watershed

Watershed characteristics	Results obtained
Relief typology	Weak

These results show that the basin is very small with an elongated shape and low relief.

The average permeability coefficient (km) is equal to 3.66731.10-6, so the permeability of the soil is low.

The particle size curves in Figure 15 represent the results of the particle size test carried out on the seven (7) samples.
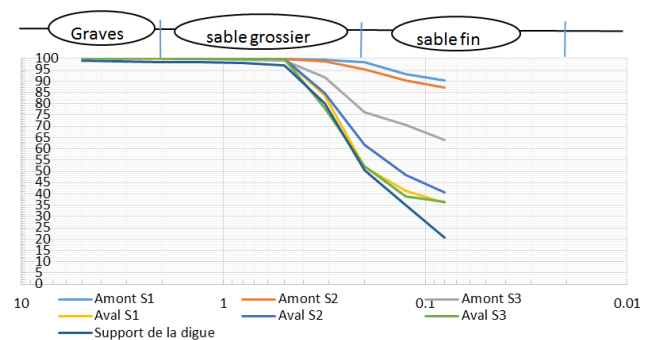
Figure 15. *Particle size curves on the seven (7) samples.*

The particle size curves do not allow a good classification of the soil due to the absence of the parameters D10, D30 and D60. It was therefore necessary to carry out the particle size test by sedimentometry. The results of the Cc and Cu calculations are presented in Table 5.

Table 5. *Curvature and uniformity coefficients.*

Samples	Curvature coefficient (Cc)	Uniformity coefficient (Cu)
Upstream S1	4,20	6,20
Upstream S2	6,30	10,17
Upstream S3	4,65	8,33
Downstream S1	0,39	4,62
Downstream S2	0,55	4,88
Downstream S3	0,39	4,62
Embankment of the dike	1,15	4,62

The uniformity coefficients of all samples are greater than 2, so the grain size of the soil is spread out. The curvature coefficients of the upstream and downstream samples are not between 1 and 3, so the soil is poorly graded upstream and downstream of the dike. On the other hand, the coefficient of curvature of the dike backfill sample is between 1 and 2 so the

grain size of the dike backfill is well graded.

The results of the tests on the specific weight are given in table 6.

Table 6. Results of specific weights of solid grains.

Samples	γ$_s$ moyen (g/ml)
Upstream S3	2,649
Downstream S1	2,622
Downstream S2	2,927
Downstream S3	2,653
Embankment of the dike	2,613

Average γs is greater than 2.6 g/ml so the soil contains heavy particles. The results of the methylene blue tests are presented in Table 7.

Table 7. Results of the methylene blue test.

Samples	VBS
Upstream S3	1,12
Downstream S1	0,71
Downstream S2	0,71
Downstream S3	0,56
Embankment of the dike	0,81

The VBS values are in the interval [0.2; 1.5] therefore the soil is sandy-loamy.

The results of the sand equivalent test carried out on samples S3 upstream, S1, S2 and S3 downstream as well as on the support soil of the dike are recorded in table 8.

Table 8. Sand equivalent results.

Samples	Sand equivalent
Upstream S3	27,07
Downstream S1	27,06
Downstream S2	42,27
Downstream S3	42,21
Embankment of the dike	53,45

The sand equivalents are less than 60 so the soil is clayey

sand. The Atterberg limits test is carried out on the upstream samples S1 and S2. Figures 16 and 17 represent the curves for determining the liquidity limit.
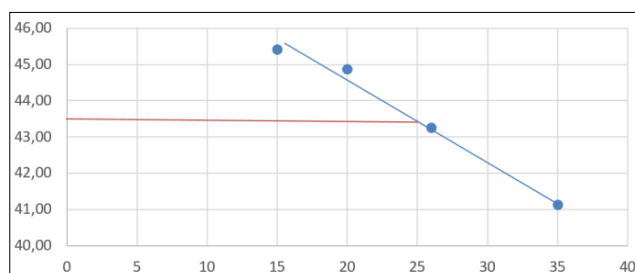
Figure 16. Curve of the liquidity limit of the upstream S1 sample.
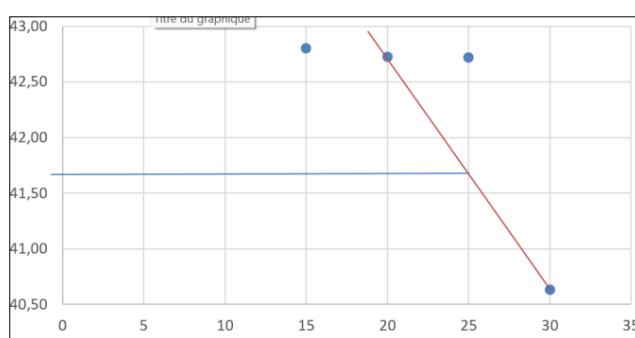
Figure 17. Curve of the liquidity limit of the upstream S2 sample.

Figures 16 and 17 give the values of the liquidity limit of upstream S1 and upstream S2 which are respectively 43.5% and 41.6%. The results of the compactness index (Ic) and the plasticity index (Ip) are presented in Table 9.

Table 9. Atterberg limit results.

Samples	Hint	
Upstream S1	Ip	17,8
	Ic	2,21
Upstream S2	Ip	25,6
	Ic	1,38

The Ip are the interval [15; 40] and the Ic > 1 therefore the soil is in a plastic and solid state.

The GTR classification was made using the results obtained in the geotechnical tests.

Samples S3 upstream, S1, S2 and S3 downstream of the dike are class A1, so they are lightly polluted fine sand. On the other hand, samples S1, S3 upstream are respectively fine clayey sand and marly clay. This can be explained by the fact that runoff water carries materials with it. The embankment is

class B2 so the soil is a slightly clayey sand.

To check the stability of the structure, it is necessary to know the cohesion and the internal friction angle of the dike backfill. Table 10 gives the normal and tangential stresses at the different loadings.

Table 10. *Results of calculations of σ_n (kPa) and τ (kPa).*

Overload (kg)	σₙ (kPa)	τ (kPa)
4	237,819	87,582
8	514,370	305,999
16	1023,195	282,611

Figure 18 shows the shear stress-deformation curve plotted using Table 10.
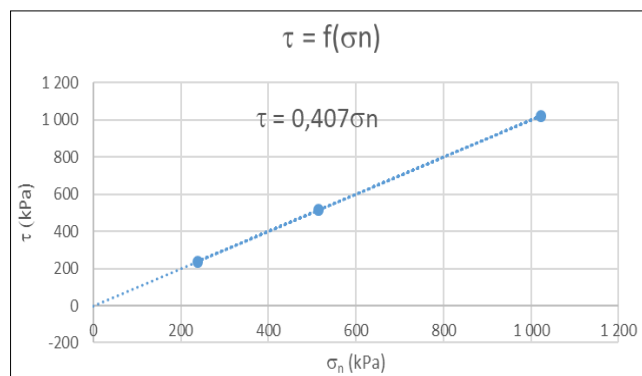

Figure 18. *Shear force-strain curve.*

The cohesion and friction angle are given in table 11.

Table 11. *Cohesion and angle of internal friction.*

Cohesion	C(kPa)	0
Internal friction angle	φ (°)	21,82

The cohesion is zero, which confirms that the backfill is made with sand.

Figures 19 and 20 respectively give the variation in the moving average of annual rainfall and the variation in the moving average of daily maximum rainfall.
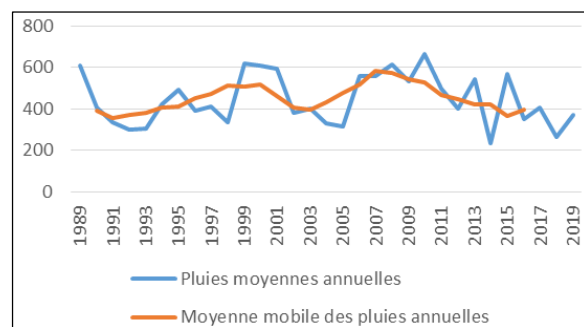
Figure 19. *Variation in the moving average of annual rainfall.*
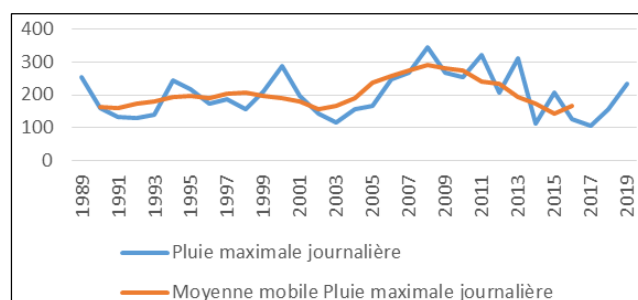
Figure 20. *Variation in the moving average of daily maximum rainfall.*

The analysis of this data did not show any doubtful periods. Therefore, these data will be used for the diagnosis of the dimensioning of the work.

The graphic adjustment of the daily maximum data by Gumbel's law made it possible to obtain the graph in Figure 21.
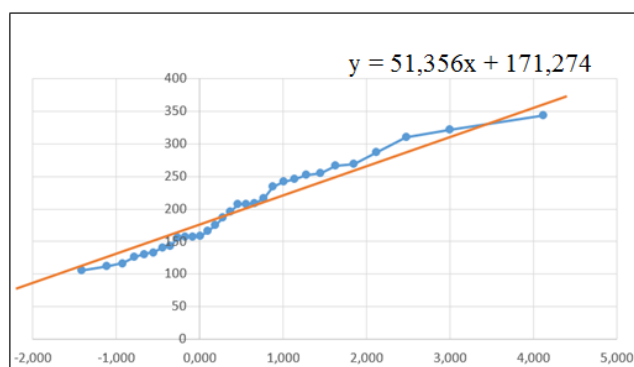
Figure 21. *Graphical adjustment of daily maximum rainfall.*

The analysis of Figure 21 reveals that there is a distribution of the cloud of points around the adjustment line. Thus the results of the parameters obtained by the graphical method will be used as input parameters for the design of the structure. Table 12 gives the values of Gumbel's law (s and X0) obtained by the graphical method.

Table 12. Gumbel Settings by Graphical Adjustment.

δ (écart type)	a	moyenne	X₀	s
65,841	0,019	200,906	171,274	51,356

The results obtained by the moment method are reported in Table 13.

Table 13. Gumbel Parameters by Adjustment by the Moment Method.

δ (écart type)	moyenne	s	X₀
65,841	200,906	51,356	171,274

The scale factor and the amount of rainfall in the current state are the same in both methods.

For the estimation of the flow by the ORSTOM method, since the area of the catchment area is 3.72 km² also the smallest height of precipitation is equal to 234.9 mm and the largest 664.4 mm, so all heights are in the interval [150; 1600]. The decadal flow calculations by the ORSTOM method are given in Table 14.

Table 14. Calculation of Qr10 by the ORSTOM method.

A	0,91
P_{10}	286,844
P_{100}	407,521
K_{r10}	24
Pan	441,24
S	3,72
α_{10}	2,6
Tb_{10}	440
Q_{r10} (m³/s)	23,17

For the ORSTOM method, the ten-year flood amounts to 23.17 m3/s.

For the estimation of the flow by the CIEH method, since the catchment area is 3.72 km² so it is in the range [0.07; 2,500] also the smallest height is equal to 234.9 mm and the largest 664.4 mm, so all heights are in the interval [150; 1600]. The results of the calculations are recorded in Table 15.

Table 15. Calculation of Q10 by the CIEH method.

Pan	441,24
S	3,72
I_g	5,98
Q_{10} (m³/s)	13,86

For the CIEH method, the ten-year flood is equal to 13.86m3/s.

Table 16 presents the results of the centennial flow calculation or project flood.

Table 16. Project Flood Calculation.

	Q_{10} (m³/s)	C	Q_{100} (m³/s)
ORSTOM	23,17		54,99
CIEH	13,86	2,37	32,89

For safety reasons, the maximum ten-year flood Q100 = 54.99 m3/s is used as the project flow.

To make the diagnosis of the dike, it is necessary to compare the dimensions found on site with the results of the resizing. Tables 17 and 18 show the dimensions of the dike found at the site and the results of the dike resizing, respectively.

Table 17. Dimensions of the dike.

Ridge width Lc (m)	7,02
Width of the base of the dike Lb (m)	58,8
Height of the dike H (m)	2,88
Water Slide h (m)	0,7
Height of the reservoir Hr (m)	2,27
Length of weir (m)	30,00

Table 18. Resizing the dike.

Wind speed (u in km/h)	15,24
TN Rating (m)	75,06
Lengths of the (m)	132
FETCH Length (Lf in m)	0,12
Wave height (Hv in m)	0,79
Wave propagation speed (v in m/s)	3,09

Revenge (R in m)	1,08
Height of the dike (Hd in m)	3,00
Ridge width (Lc in m)	2,86
Width of the base of the dike (Lb in m)	14,86
Water Gap (h in m)	0,70
Height of the reservoir (Hr in m)	1,22
Flow coefficient (m)	0,40
Project flood (Q in m3/s)	54,99
Spillway length (L in m)	52,99

The resizing showed that the dimensions of the dike are acceptable except for the length of the spillway. The calculation results for the LANE rule check are shown in Table 19.

Table 19. Checking for infiltration under the dike.

L_v (m)	L_H (m)	C	H_r (m)	$L_V + \frac{1}{3} * L_H \geq C * H_r$
58,81	132	7	1,22	vérifié

The LANE rule is respected, so the risk of infiltration under the dike is eliminated.

The results for the protection of the upstream slope are given in Table 20.

Table 20. Calculation of the thickness of the upstream slope protection.

Y	Pente	C	V (m/s)	e (m)
2,8	1/2	0,026	3,09	0,24

For good protection of the upstream slope, the thickness of the protective layer had to be equal to 24 cm, but the protective layer found on the site is 15 cm. So the protection of the upstream slope is not good. The protection of the downstream embankment is made of perré with a thickness of 20 cm, which complies with the standard which requires a thickness of at least 16 cm, so it is acceptable. The ridge protection is made of laterite with a thickness of 16 cm, which is below the standard. The thickness of the laterite layer should be at least 20 cm. So the protection of the ridge is not good.

The results of the slip stability calculations are given in Table 21.

Table 21. Calculation of Slip Stability.

W_1	U	P_a	F_{SG}
179,69	205,8	2,45	1,84

$F_{SG} = 1,84 \geq 1,5$ Slip stability is checked.

The results of the rollover stability calculations are given in Table 22.

Table 22. Calculation of Rollover Stability.

$\sum$M Stabilizers	530,39
$\sum$M Stunning	4035,53
F_{SR}	0,13

$F_{SR} = 0,13 < 1,5$ Rollover stability is not checked.

In summary, the diagnosis of the dike failure according to the three hypotheses raised yielded:

3.1. Excess Flooding

Taking the average annual precipitation of 1989 (609.9 mm), which returns ten years later in 1999 (618.5 mm), as a reference point, the rupture may be due to an excess of flooding since in 2010, the average rainfall was well above the reference threshold, reaching 664.4 mm. So the rupture may be due to an excess of flooding.

3.2. External Erosion

To minimize the risk of breakage, good slope protection is necessary. However, the protection of the upstream slope, which was supposed to be 24 cm thick, is 15 cm. Similarly, the thickness of the laterite layer of the ridge which must have been 20 cm is 16 cm. So the protections at the crest and the upstream embankment are not good. If slope protection is not adequate, water can seep into the embankment, which can cause erosion. In this context, it is relevant to speak of external erosion, since the protection of the downstream slope is sufficient.

3.3. Undersizing

The sizing is acceptable except for the length of the spillway. Also, the overturning stability is not checked, which can be a cause of breakage.

4. Conclusion

There are many shortcomings in the design of the Keur

Bara KAIRE dike. First there is the excess flooding, then the poor protection of the embankments and finally the undersizing. This confirms the hypotheses outlined above. Therefore, to solve the flooding problems caused by the failure of the dike, it is first proposed to redo the structure using a homogeneous earthen dike with zones with a slope of 1/2 upstream and downstream, clay sand for the backfill to prevent water infiltration, a protective layer of 24 cm for the upstream embankment, 20 cm for the crest and 15 cm for the downstream embankment and for more resistance, build 50 cm thick ramming walls with a length of 1 m for the anti-fox screen. Table 23 presents the results of the design of the flanking walls.

Table 23. Dimensioning of the flanking walls.

Peak Width (m)	2,86
Height of the wall above the TN (m)	3
Wall thickness (m)	0,5
Length of the anti-fox screen (m)	1
Slope of side walls	1/2 (Upstream and downstream)

It is essential to consider that this article is not limited to the simple rehabilitation of the dike.

In order to guarantee the sustainability of the structure, it would be wise for the stakeholders to work together to develop an organizational plan dedicated to monitoring, control and maintenance. This will establish a solid structure that will ensure the long-term preservation of the structure.

Abbreviations

℃	Degree Celsius
ANACIM	National Agency for Civil Aviation and Meteorology
ANSD	National Agency for Statics and Demography
Cc	Curvature Coefficient
CIEH	Inter-African Committee for Hydraulic Studies
cm	Centimeter
Cu	Uniformity Coefficient
D10	Sieve Diameter Corresponding to 10%
D30	Sieve Diameter Corresponding to 30%
D60	Sieve Diameter Corresponding to 60%
Dd	Drainage Density
Ds	Specific Elevation
ES	Sand Equivalent
Fd	Exceeding Frequency
Fnd	Frequency of Non-exceeding
FSG	Slip Safety Factor
FSR	Rollover Safety Factor
GNSS	Global Navigation Satellite Systems
GPS	Global Positioning System
GTR	Guide to Road Earthworks
HD	Height of the Dike
Hr	Height of the Reservoir
Ic	Consistency Index
Ig	Overall Slope Index
Ip	Plasticity Index
k	Permeability Coefficient
KG	Shape Index
Km	Kilometer
km²	Square Kilometer
L	Length of the Equivalent Rectangle
Lb	Base Width of the Dike
Lc	Ridge Width
m	Meter
DEM	Digital Terrain Model
MRUH	Ministry of Urban Renewal and Housing
NF	French Standard
ORSTOM	Overseas Scientific and Technical Research Office
P	Perimeter of the Watershed
P10	Ten-year Daily Rain
P100	100-year Daily Rain
PVC	Polyvinyl Chloride
Q100	Centennial Flow or Design Flood
Qr10	Ten-year Flow
A	Free Revenge
s	Second
S	Watershed Area
T	Return Period
TN	Natural Terrain
U	Reduced Gumbel Variable
UFR-SI	Engineering Sciences Training and Research Unit
VBS	Methylene Blue Value
w	Water Content
WL	Liquidity Limit
WP	Plasticity Limit
Zd	Setting Dimension

Conflicts of Interest

The authors declare no conflicts of interest.

References

[1] ANSD, «Projection of the population of the Thiès region» 2022.

[2] C. Sophie and L. Jean, "Drinking water service: From the logic of supply to the control of demand," Jwarp, 1996. Concrete dikes. [Performance]. 2020.

[3] I. SEYE, Design of a rainwater sanitation network integrated into a geographic information system in the Sampathé district, Thiès: UFR SI, 2019, p. 9.

[4]   C. MERLIN, "Drinking Supply Project for Cities in the Central and Coastal Zone. Dakar," (July 2010).

[5]   S. Faye, "Hydrodynamic modeling of the aquifers of the northern coast between Kayar and Saint-Louis. Impact of future withdrawals envisaged within the framework of the water supply of Dakar and its surroundings," Dakar, 1995.

[6]   B. Igor and G. Didier, "Tool to aid in the diagnosis of the drinking water network for the city of Chisinau by spatial and temporal analysis of hydraulic dysfunctions," jwarp, 2004.

[7]   M. AVERETTE, 2005. [Online]. Available: http://fr.scienceaq.com/

[8]   SETICO/CONCEPT, "Possible variants of water resource mobilization," 2013.

[9]   C. M. S. SONES, "Mobilization of alternative water resources for irrigation in the Dakar region. 79 p.," 2007.

[10]   M. D. KHOUSSA, "Study of the dike," at Hydrological Analysis-Diagnostic of the Sibidiang dam in the commune of Medina Gounass, UFR-SET, 2020, p. 60.